Journal of Sound and Vibration 330 (2011) 2079–2093

Contents lists available at ScienceDirect

Journal of Sound and Vibration

journal homepage: www.elsevier.com/locate/jsvi

Accurate vibration analysis of thick, cracked rectangular plates

C.S. Huang [a,*], A.W. Leissa [b], R.S. Li [a]

[a] Department of Civil Engineering, National Chiao Tung University, 1001 Ta-Hsueh Road, Hsinchu 30050, Taiwan
[b] Department of Mechanical Engineering, Colorado State University, Fort Collins, CO 80523, USA

ARTICLE INFO

Article history:
Received 29 April 2010
Received in revised form
3 November 2010
Accepted 7 November 2010
Handling Editor: S. Ilanko
Available online 7 December 2010

ABSTRACT

This work applies the Ritz method to accurately determine the frequencies and nodal patterns of thick, cracked rectangular plates analyzed using Mindlin plate theory. Two types of cracked configuration are considered, namely, side crack and internal crack. To enhance the capabilities of the Ritz method in dealing with cracked plates, new sets of admissible functions are proposed to represent the behaviors of true solutions along the crack. The proposed admissible functions appropriately describe the stress singularity behaviors around a crack tip and the discontinuities of transverse displacement and bending rotations across the crack. The present solutions monotonically converge to the exact frequencies as upper bounds when the number of admissible functions increases. The validity and accuracy of the present solutions are confirmed through comprehensive convergence studies and comparison with the published results based on the classical thin plate theory. The proposed approach is further employed to investigate the effects of the length, location, and orientation of crack on frequencies and nodal patterns of simply supported and cantilevered cracked rectangular plates. The results shown are the first ones available in the published literature.

1. Introduction

A plate may be ceaselessly subjected to an irregular load induced by waves or subjected to a cyclic load induced by a machine, and fatigue cracks may be finally initiated. A crack in a plate can make its dynamic characteristics significantly different from those for an intact plate. Hence, it is important to clarify the dynamic characteristics of cracked plates.

Although static analyses of cracked plates (i.e., determining stress intensity factors) have intensively been performed, investigations of their free vibrations are rather little. Most of these works considered thin plates and employed the classical thin plate theory. To solve for vibrations of cracked rectangular thin plates with simply supported conditions at all edges or two opposite edges and having cracks parallel to one of the edges, Lynn and Kumbasar [1], Stahl and Keer [2], Aggarwala and Ariel [3], Neku [4], and Solecki [5] applied different techniques on establishing integral equations, while Hirano and Okazaki [6] established their solutions starting from Levy's solution and fitting the mixed boundary conditions on the line of the crack by means of a weighted residual method. Qian et al. [7] and Krawczuk [8] proposed a stiffness matrix for the element with crack in a finite element solution. Yuan and Dickinson [9] and Liew et al. [10] employed the Ritz method in conjunction with different domain decomposition techniques. Huang and Leissa [11] used the Ritz method with thin plate theory and proposed a new set of admissible functions for rectangular plates with side cracks. Bachene et al. [12] applied the extended finite element method to analyze the free vibrations of thin rectangular plates with horizontal cracks. Ma and Huang [13] simply

* Corresponding author.
E-mail addresses: cshuang@mail.nctu.edu.tw, cshuang@cc.nctu.edu.tw (C.S. Huang), awleissa@mindspring.com (A.W. Leissa).

0022-460X/$ - see front matter © 2010 Elsevier Ltd. All rights reserved.
doi:10.1016/j.jsv.2010.11.007

used the commercial finite element computer program ABAQUS and selected eight-node two-dimensional shell elements (S8R5) to determine natural frequencies of cantilevered thin plates with horizontal or vertical side cracks to verify the correctness of their experimental results.

Several experiment works on vibrations of thin, cracked plates were reported. Maruyama and Ichinomiya [14] employed the real-time technique of time averaged holographic interferometry to determine the natural frequencies and corresponding mode shapes of clamped rectangular thin plates with straight cracks. Ma and Huang [13] and Ma and Hsieh [15] utilized the amplitude fluctuation electronic speckle pattern interferometry to determine the natural frequencies and corresponding mode shapes of cantilevered rectangular thin plates with horizontal or vertical side cracks.

Very little published research is available about the vibrations of thick, cracked plates. Based on the simplified Reissner theory, Lee and Lim [16] used the Ritz method with a domain decomposition technique to determine the fundamental frequencies of center-cracked rectangular plates with simply support conditions.

The purpose of the present paper is twofold: (1) to propose sets of admissible functions for the Ritz method to deal with a straight crack in a thick plate, using the Mindlin plate theory; (2) to provide new accurate natural frequencies of cracked plates with moderate thickness for expanding the currently available data base. The Ritz method has been popular in analyzing free vibrations of plates with simple geometry because of its simplicity in formulation and rigorous mathematic background. The available solutions using the Ritz method for cracked rectangular plates cooperates with various domain decomposition techniques (i.e., [9,10,16]). These solutions lose an important property of the Ritz method in providing monotonically convergent upper-bound solutions for vibration frequencies because the admissible functions are not continuous everywhere along the interconnecting boundaries between two adjacent sub-domains or because artificial springs are installed along the interconnecting boundaries, and the accuracy of solutions depend on whether the springs are stiff enough or not. To remedy the main drawback of these solutions, the present paper investigates the vibrations of thick plates with side cracks and internal cracks and proposes new sets of admissible functions that properly describe the stress singularity behaviors at the neighborhood of a crack tip and show the discontinuities of transverse displacement and bending rotations across the crack.

The validity and correctness of the proposed solution are confirmed by convergence studies and comparison with the published results. The proposed methodology is further applied to investigate the effects of the length, position, and inclination angle of crack on the vibration frequencies of simply supported and cantilevered cracked rectangular plates with thickness to side length ratio equal to 1/10. Accurate frequencies are tabulated and some corresponding nodal patterns are also shown for the first five modes. The results shown are the first ones available in the published literature.

2. Methodology

Two types of cracked configuration are considered, namely, side crack and internal crack. The geometry and dimension of a cracked rectangular plate are shown in Figs. 1 and 2. The natural frequencies of the cracked plates are determined via the famous Ritz method using Mindlin plate theory. For the free vibration of a plate in Cartesian coordinates (x, y), the energy functional in the Ritz method is defined as

$$\Pi = V_{\max} - T_{\max}, \tag{1}$$

where the maximum strain energy ($V_{\max}$) and the maximum kinetic energy ($T_{\max}$) are [17]

$$V_{\max} = \iint_A \frac{D}{2}\left\{\left[\psi_{x,x}^2+\psi_{y,y}^2+2\upsilon\psi_{x,x}\psi_{y,y}+\frac{1-\upsilon}{2}(\psi_{x,y}+\psi_{y,x})^2\right]\right\}+\frac{\kappa^2 Gh}{2}\left[(\psi_x+w_{,x})^2+(\psi_y+w_{,y})^2\right]\mathrm{d}A, \tag{2}$$

$$T_{\max} = \frac{\omega^2}{2}\iint_A\left\{\rho h w^2+\frac{\rho h^3}{12}(\psi_x^2+\psi_y^2)\right\}\mathrm{d}A, \tag{3}$$

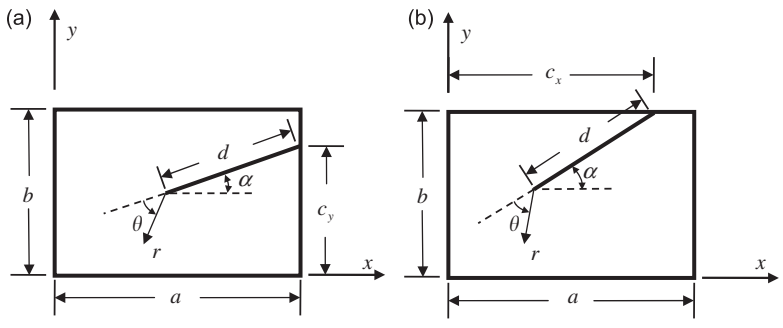

Fig. 1. Dimensions and coordinates for a rectangular plate with a side crack: (a) a plate with a crack intersecting $x=a$ and (b) a plate with a crack intersecting $y=b$.

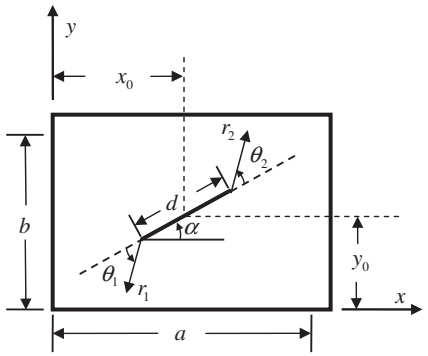

Fig. 2. Dimensions and coordinates for a rectangular plate with an internal crack (x_0 and y_0 locate the center of the crack).

where w is the transverse displacement of the mid-plane; ψ_x and ψ_y are the bending rotations of the mid-plane normal in the x and y directions, respectively; h is the thickness of the plate; $D=Eh^3/12(1-\upsilon^2)$ is the flexural rigidity; E is the modulus of elasticity; υ is Poisson's ratio ; κ^2 is the shear correction factor and set to $\pi^2/12$; G is the shear modulus; ρ is the mass density of the plate; ω is a free vibration frequency, and the subscript comma denotes partial derivative with respect to the coordinate defined by the variable after the comma. The vibration frequencies of the plate are obtained by minimizing the energy functional.

In Eqs. (2) and (3), $w(x,y)$, $\psi_x(x,y)$ and $\psi_y(x,y)$ are approximated by finite series of admissible functions, which must satisfy the geometric boundary conditions under consideration, and are expressed as

$$\psi_x=\Phi_{1p}+\Phi_{1c},\quad \psi_y=\Phi_{2p}+\Phi_{2c},\quad w=\Phi_{3p}+\Phi_{3c}, \tag{4}$$

where Φ_{kp} (k=1, 2 and 3) consist of algebraic polynomials, and Φ_{kc} (k=1, 2 and 3) consist of special functions, which account for the singular behaviors of moments and shear forces at a crack tip and are discontinuous across the crack. These special functions are simply called crack functions in the following.

In Eqs. (4) Φ_{kp} are expressed as

$$\Phi_{kp}(x,y)=\sum_{i=1,2}^{I_k}\sum_{j=1,2}^{J_k}A_{ij}^{(k)}P_{ki}(x)Q_{kj}(y), \tag{5}$$

where $P_{ki}(x)$ and $Q_{kj}(y)$ (k=1, 2 and 3) are sets of orthogonal polynomials in the x and y directions of the rectangular plate under consideration (Figs. 1 and 2), respectively. These orthogonal polynomials are generated by using a Gram–Schmidt process [18] and satisfy the geometrical boundary conditions of the rectangular plate. These polynomials construct functions which become mathematically complete if infinite terms are used. Notably, using orthogonal polynomials results in considerably less ill-conditioning of the matrix than using ordinary polynomials.

The polynomials in Eqs. (5) are continuous and are not singular anywhere in the domain under consideration. To enhance the capabilities of the Ritz method on dealing with cracked plates, one needs other admissible functions to help the Ritz method to recognize the existence of a crack. The asymptotic solutions at the neighborhood of the crack tip are usually good candidates for these admissible functions. According to Huang [19] in considering moment singularities at the neighborhood of the crack tip, the asymptotic solutions for the bending rotations and transverse displacement in a polar coordinate system are

$$\psi_{ra}(r,\theta)=(A_1\cos(\lambda+1)\theta+A_2\sin(\lambda+1)\theta+A_3\cos(\lambda-1)\theta+A_4\sin(\lambda-1)\theta)r^{\lambda}, \tag{6a}$$

$$\psi_{\theta a}(r,\theta)=(A_2\cos(\lambda+1)\theta-A_1\sin(\lambda+1)\theta+k_2A_4\cos(\lambda-1)\theta-k_2A_3\sin(\lambda-1)\theta)r^{\lambda}, \tag{6b}$$

$$w_a(r,\theta)=(C_1\cos(\lambda+1)\theta+C_2\sin(\lambda+1)\theta+\gamma_1A_3\cos(\lambda-1)\theta+\gamma_1A_4\sin(\lambda-1)\theta)r^{\lambda+1}, \tag{6c}$$

where

$$k_2=-\frac{[2(1-\upsilon)+(1+\upsilon)(\lambda+1)]}{[2(1-\upsilon)-(1+\upsilon)(\lambda-1)]},\quad \gamma_1=\frac{\upsilon-1}{-3+\lambda+\upsilon+\upsilon\lambda},$$

where λ and coefficients A_i and C_j (i=1, 2, 3, 4 and j=1, 2) are determined from the boundary conditions along the crack. For the free edges of the crack it is found that $\lambda=n/2$ (n=1, 2, 3,…) and the relations between coefficients A_i and C_j are given in Huang [19]. When considering shear force singularities around the crack tip, one can find the asymptotic solutions

$$\psi_{ra}(r,\theta)=[\overline{A}_1\cos\overline{\lambda}\theta+\overline{A}_2\sin\overline{\lambda}\theta+\overline{A}_3\cos(2+\overline{\lambda})\theta+\overline{A}_4\sin(2+\overline{\lambda})\theta]r^{\overline{\lambda}+1}, \tag{7a}$$

$$\psi_{\theta a}(r,\theta)=[\overline{B}_1\cos\overline{\lambda}\theta+\overline{B}_2\sin\overline{\lambda}\theta+\overline{A}_4\cos(2+\overline{\lambda})\theta-\overline{A}_3\sin(2+\overline{\lambda})\theta]r^{\overline{\lambda}+1}, \tag{7b}$$

$$w_a(r,\theta)=[\bar{l}_1(\overline{A}_1\cos\overline{\lambda}\theta+\overline{A}_2\sin\overline{\lambda}\theta)+\bar{l}_2(\overline{B}_2\cos\overline{\lambda}\theta-\overline{B}_1\sin\overline{\lambda}\theta)]r^{\overline{\lambda}}, \tag{7c}$$

where

$$\bar{l}_1=\frac{-D}{2\kappa^2Gh}(3-\upsilon+(1+\upsilon)(1+\overline{\lambda})),\quad \bar{l}_2=\frac{D}{2\kappa^2Gh}(2(1-\upsilon)-(1+\upsilon)\overline{\lambda}),$$

$\overline{\lambda}=n/2$ (n=1, 2, 3,…) and the relations between coefficients $\overline{A}_1$,$\overline{A}_2$,$\overline{A}_3$,$\overline{A}_4$,$\overline{B}_1$, and $\overline{B}_2$ are also given in Huang [19].

But, it is complicated to introduce the asymptotic solutions given in Eqs. (6) and (7) into the admissible functions. Instead, the following, much less complicated, set of crack functions is proposed for admissible functions:

$$\left\{r^{(2n-1)/2}\cos\frac{2l+1}{2}\theta \text{ and } r^{(2n-1)/2}\sin\frac{2l+1}{2}\theta|,\quad l=0,\,1,\,2,\ldots,n \text{ and } n=1,2,\,3,\ldots\right\}. \tag{8}$$

Apparently, the asymptotic solutions given in Eqs. (6) and (7) for λ and $\overline{\lambda}$ equal to $(2k+1)/2$ (k=0,1,2,…) can be linearly expanded into this new set of crack functions. In Eqs. (6), ψ_{ra} and $\psi_{\theta a}$ are linear combinations of $r^{\lambda}\cos(\lambda+1)\theta$, $r^{\lambda}\sin(\lambda+1)\theta$, $r^{\lambda}\cos(\lambda-1)\theta$, and $r^{\lambda}\sin(\lambda+1)\theta$, which are included in the set of functions in Eq. (8). Similar situations happen to w_a in Eq. (6c) and the asymptotic solutions in Eqs. (7). For plates with side cracks (see Fig. 1), Φ_{kc} in Eq. (4) are expressed as

$$\Phi_{kc}(r,\theta)=g_k(x,y)\left(\sum_{n=1}^{\overline{N}_{1k}}\sum_{l=0}^{n}B_{nl}^{(k)}r^{(2n-1)/2}\cos\frac{2l+1}{2}\theta+\sum_{n=1}^{\overline{N}_{2k}}\sum_{l=0}^{n}C_{nl}^{(k)}r^{(2n-1)/2}\sin\frac{2l+1}{2}\theta\right)\qquad(\text{for } k=1,\,2,\,3), \tag{9}$$

where functions $g_k(x,y)$ are inserted to satisfy the geometric boundary conditions along the edges of a rectangular plate.

When plates with internal cracks (Fig. 2) are under consideration, Eq. (9) is not suitable for the admissible functions. There are two crack tips, so one needs admissible functions that can properly describe the singularity behaviors around both tips. Hence, the following admissible functions are proposed:

$$\begin{aligned}\Phi_{kc}=g_k(x,y)\Bigg\{&\sum_{n=1}^{\overline{N}_{1k\_1}}\sum_{l=0}^{n}B_{nl}^{(k)}r_1^{(2n-1)/2}\cos\frac{2l+1}{2}\theta_1+\sum_{n=1}^{\overline{N}_{1k\_2}}\sum_{l=0}^{n}\tilde{B}_{nl}^{(k)}r_2^{(2n-1)/2}\cos\frac{2l+1}{2}\theta_2\\&+r_2^{\beta}\sin^2(\theta_2/2)\sum_{n=1}^{\overline{N}_{2k\_2}}\sum_{l=0}^{n}C_{nl}^{(k)}r_1^{(2n-1)/2}\sin\frac{2l+1}{2}\theta_1+r_1^{\beta}\sin^2(\theta_1/2)\sum_{n=1}^{\overline{N}_{2k\_2}}\sum_{l=0}^{n}\tilde{C}_{nl}^{(k)}r_2^{(2n-1)/2}\sin\frac{2l+1}{2}\theta_2\Bigg\},\end{aligned} \tag{10}$$

where the origins of coordinates (r_1,θ_1) and (r_2,θ_2) are at the two crack tips, respectively, (see Fig. 2). Since $\sin(((2l+1)/2)\theta_1)$ are discontinuous at $\theta_1=\pm\pi$, $\sin^2(\theta_2/2)$ is multiplied to these functions to ensures that the resulting functions are continuous along the segment of $\theta_2=0$. Furthermore, $\sin^2(\theta_2/2)$ is symmetric with respect to $\theta_2=0$ so that it does not change the symmetry feature of $\sin(((2l+1)/2)\theta_1)$. That means $\sin^2(\theta_2/2)\sin(((2l+1)/2)\theta_1)$ are still anti-symmetric with respect to the line including the crack. Because the first derivatives of $\sin^2(\theta_2/2)$ with respect to x and y yield another singularity at $r_2=0$, r_2^{β} with $\beta\geq 0.5$ is multiplied by $\sin^2(\theta_2/2)$ to avoid yielding incorrect singular behaviors for stress resultants at $r_2=0$. Similar situations are also applied to $\sin(((2l+1)/2)\theta_2)$ terms. In the following analyses, β=1.5 is used so that no moment and shear singularities will result from $r_i^{\beta}\sin^2(\theta_i/2)$ (i=1 and 2).

For simplicity of notation, I_k and J_k (k=1, 2, 3) in Eq. (5) are set equal to I and J, respectively, and $\overline{N}_{1k}$ and $\overline{N}_{2k}$ in Eq. (9) are set equal to $\overline{N}$ when considering a rectangular plate with a side crack. Substituting Eqs. (5) and (9) into Eqs. (1)–(3) and minimizing the energy functional Π with respect to coefficients $A_{ij}^{(k)}$, $B_{nl}^{(k)}$ and $C_{nl}^{(k)}$ yields $3IJ+3\overline{N}(\overline{N}+3)$ linear algebraic equations for those coefficients to be determined, and results in an eigenvalue problem with the eigenvalues describing the natural frequencies of plate. Similarly, when considering a rectangular plate with an internal crack, one sets all $\overline{N}_{1k\_1}$, $\overline{N}_{1k\_2}$, $\overline{N}_{2k\_1}$, and $\overline{N}_{2k\_2}$ (k=1, 2, 3) in Eq. (10) equal to $\overline{N}$. Then, one obtains $3IJ+6\overline{N}(\overline{N}+3)$ linear algebraic equations for those coefficients to be determined, and an eigenvalue (frequency) determinant of this same order.

3. Convergence studies

The Ritz method always gives upper bounds on vibration frequencies, and these upper-bound solutions converge to the exact solution as the number of appropriate admissible functions increases sufficiently. This important feature provides an excellent way to verify the correctness of the proposed solutions. Convergence studies of side-cracked and internal-cracked rectangular plates were carried out herein to confirm the accuracy of the present solutions. Poisson's ratio for the plate material is set equal 0.3 for all the results shown here.

In the present section and the following section, simply supported and cantilevered plates are under investigation. The geometric boundary conditions for a simply supported plate are

$$\begin{aligned}&\psi_x(x,0)=0,\quad \psi_x(x,b)=0,\quad \psi_y(0,y)=0,\quad \psi_y(a,y)=0,\\&w(x,0)=0,\quad w(x,b)=0,\quad w(0,y)=0,\quad w(a,y)=0.\end{aligned} \tag{11}$$

Accordingly, to make the admissible functions in Eq. (9) satisfy the geometric boundary conditions of simple support, the following $g_k(x,y)$ (k=1, 2, 3) are simply used:

$$g_1(x,y)=y(b-y), \quad g_2(x,y)=x(a-x), \text{ and } g_3(x,y)=xy(a-x)(b-y). \tag{12}$$

The cantilevered plates are clamped at the edge with x=0, and $g_k(x,y)$ (k=1, 2, 3) are set as

$$g_k(x,y)=x.$$

3.1. Side-cracked plates

Table 1 presents the convergence studies of a simply supported rectangular thin plate (a/b=2 and h/b=0.01) having a horizontal side crack at c_y/b=0.5 with a length of d/a=0.5 (Fig. 1a), while Table 2 shows the convergence studies of a plate with

Table 1
Convergence of frequency parameters $\omega a^2\sqrt{\rho h/D}$ for a simply supported rectangular plate with a horizontal side crack ($a/b=2.0$, $c_y/b=0.5$, $d/a=0.6$, $h/b=0.01$), as in Fig. 1a.

Mode no.	No. of corner function ($\overline{N}$)	Order of polynomial ($I\times J$)						Published results
		5×5	6×6	7×7	8×8	9×9	10×10	
1(S)	0	49.35	49.34	49.34	49.34	49.34	49.34	[36.17]
	1	49.30	49.29	49.28	49.28	49.27	49.27	(37.44)
	2	42.49	42.23	39.92	39.78	38.52	38.46	
	3	36.85	36.60	36.45	36.38	36.32	36.29	
	4	36.24	36.20	36.16	36.16	36.14	36.14	
	5	36.16	36.15	36.14	36.14	36.13	36.13	
	6	36.15	36.14	36.13	36.13	36.12	36.12	
	7	36.14	36.13	36.12	36.12	36.11	36.11	
	8	36.13	36.12	36.11	36.11	36.10	36.10	
2(A)	0	79.04	79.03	78.93	78.93	78.93	78.93	[57.49]
	1	79.01	79.00	78.89	78.89	78.89	78.89	(59.31)
	2	76.06	75.95	75.21	75.17	74.88	74.86	
	3	70.36	68.74	68.02	67.63	67.36	67.07	
	4	57.93	57.75	57.69	57.65	57.63	57.61	
	5	57.45	57.40	57.39	57.37	57.37	57.35	
	6	57.40	57.37	57.37	57.36	57.35	57.34	
	7	57.37	57.36	57.35	57.33	57.33	57.31	
	8	57.36	57.34	57.34	57.32	57.31	57.30	
3(S)	0	164.2	129.5	129.5	128.2	128.2	128.2	[72.59]
	1	164.1	129.5	129.5	128.2	128.2	128.2	(72.62)
	2	148.4	129.3	129.3	128.1	128.1	128.1	
	3	74.04	73.84	73.51	73.43	73.27	73.23	
	4	72.87	72.77	72.66	72.66	72.62	72.62	
	5	72.65	72.55	72.54	72.54	72.53	72.53	
	6	72.60	72.54	72.53	72.53	72.53	72.53	
	7	72.58	72.53	72.53	72.53	72.52	72.52	
	8	72.57	72.53	72.52	72.52	72.52	72.52	
4(S)	0	168.3	168.3	167.7	167.7	167.7	167.7	[121.3]
	1	167.7	167.5	166.8	166.7	166.6	166.5	(121.0)
	2	162.9	143.3	142.0	138.3	137.1	134.0	
	3	137.3	125.2	124.0	123.3	122.7	122.6	
	4	122.6	122.0	121.9	121.6	121.5	121.5	
	5	122.0	121.7	121.4	121.3	121.3	121.3	
	6	121.9	121.5	121.2	121.2	121.2	121.2	
	7	121.8	121.4	121.2	121.2	121.2	121.2	
	8	121.8	121.3	121.2	121.2	121.2	121.2	
5(A)	0	197.8	197.8	197.2	197.2	197.2	197.2	[141.4]
	1	197.4	197.3	196.6	196.5	196.5	196.4	(145.8)
	2	186.0	184.7	184.0	183.2	183.1	182.6	
	3	177.9	177.4	176.9	176.7	176.6	176.4	
	4	169.9	165.7	163.4	162.5	161.9	161.3	
	5	142.4	142.1	141.9	141.7	141.6	141.6	
	6	141.7	141.6	141.5	141.4	141.4	141.4	
	7	141.4	141.3	141.3	141.3	141.3	141.2	
	8	141.3	141.3	141.3	141.2	141.2	141.2	

Note: [ ]: results from Stahl and Keer [2]; ( ): results from Liew et al. [10].

Table 2
Convergence of frequency parameters $\omega a^2\sqrt{\rho h/D}$ for a simply supported rectangular plate with a horizontal side crack ($a/b=2.0$, $c_y/b=0.5$, $d/a=0.6$, $h/b=0.1$), as in Fig. 1a.

Mode no.	No. of corner functions ($\overline{N}$)	Order of polynomial ($I\times J$)					
		5×5	6×6	7×7	8×8	9×9	10×10
1(S)	0	48.27	48.26	48.26	48.26	48.26	48.26
	1	44.88	44.87	44.34	44.33	43.85	43.84
	2	35.32	35.27	35.04	35.02	34.91	34.90
	3	34.70	34.68	34.58	34.57	34.51	34.51
	4	34.51	34.49	34.45	34.44	34.42	34.41
	5	34.46	34.44	34.41	34.41	34.40	34.39
	6	34.42	34.41	34.39	34.39	34.38	34.38
	7	34.41	34.40	34.39	34.38	34.38	34.38
	8	34.40	34.39	34.38	34.38	34.38	34.38
2(A)	0	76.34	76.33	76.23	76.23	76.23	76.23
	1	74.71	74.68	74.39	74.38	74.20	74.19
	2	61.86	60.27	59.73	59.16	58.93	58.59
	3	54.09	53.74	53.64	53.46	53.40	53.29
	4	53.06	52.90	52.85	52.78	52.75	52.71
	5	52.83	52.74	52.72	52.68	52.67	52.66
	6	52.73	52.69	52.68	52.67	52.66	52.65
	7	52.68	52.67	52.66	52.65	52.65	52.65
	8	52.66	52.65	52.65	52.65	52.65	52.65
3(S)	0	150.7	122.4	122.4	121.4	121.4	121.4
	1	106.7	100.9	99.58	96.03	95.00	92.63
	2	71.47	71.43	71.28	71.27	71.20	71.19
	3	70.22	70.17	70.04	70.03	69.98	69.98
	4	69.83	69.81	69.77	69.76	69.75	69.74
	5	69.78	69.74	69.72	69.71	69.71	69.70
	6	69.74	69.71	69.70	69.70	69.70	69.70
	7	69.72	69.70	69.70	69.70	69.69	69.69
	8	69.72	69.70	69.69	69.69	69.69	69.69
4(S)	0	156.8	156.8	156.3	156.3	156.3	156.3
	1	150.5	122.4	122.4	121.4	121.4	121.4
	2	129.7	119.7	119.2	118.5	118.2	118.2
	3	118.8	115.1	114.8	114.5	114.4	114.4
	4	114.6	114.6	114.4	114.3	114.2	114.2
	5	114.4	114.2	114.1	114.1	114.1	114.1
	6	114.2	114.1	114.1	114.1	114.1	114.1
	7	114.2	114.1	114.1	114.1	114.1	114.1
	8	114.2	114.1	114.1	114.1	114.1	114.1
5(A)	0	182.3	182.3	181.8	181.8	181.8	181.8
	1	173.1	172.8	172.3	172.1	172.1	172.0
	2	158.5	155.9	155.5	154.3	154.1	153.4
	3	144.9	142.1	141.4	140.4	140.0	139.6
	4	129.6	128.4	128.2	127.8	127.7	127.6
	5	127.0	126.6	126.6	126.4	126.4	126.4
	6	126.4	126.3	126.2	126.2	126.2	126.2
	7	126.2	126.2	126.2	126.2	126.2	126.2
	8	126.2	126.2	126.2	126.2	126.2	126.2

the same geometry as that in Table 1 except for h/b=0.1. The convergence properties for the first five nondimensional frequency parameters $\omega a^2\sqrt{\rho h/D}$ are examined in terms of the number of admissible functions. The results were obtained using 5×5, 6×6, …,10×10 orthogonal polynomials in conjunction with sets of crack functions with $\overline{N}$=0, 1, 2, 3,…, 8 in Eqs. (9) for each of ψ_x, ψ_y and w. It should be noted that $\overline{N}$=0 means no crack function is used.

In Table 1, the results of Stahl and Keer [2] and Liew et al. [10] are also listed. Employing the classical thin plate theory, Stahl and Keer [2] developed solutions using an accurate Fredholm integration approach, while Liew et al. adopted the Ritz method in conjunction with a domain decomposition technique. Liew et al. [10] utilized the domain decomposition technique, so that they did not need any crack functions to help the Ritz method to identify the existence of a crack. However, Liew et al. [10] required the continuities of displacement and slope in a sense of integration along the interconnecting boundaries. The continuities of displacement and slope are not satisfied at every point along the interconnecting boundaries, so that their solutions are not guaranteed to be the upper-bound solutions for vibration frequencies and cannot properly describe the stress singularity behaviors around the crack tip.

Tables 1 and 2 reveal that the results obtained using polynomial admissible functions only are substantially larger than those obtained using both of polynomials and crack functions. As a matter of fact, the former converges to the exact solutions for simply supported intact plates because the Ritz method with only those polynomial admissible functions does not recognize the existence of a crack. Adding a small number of crack functions into the admissible functions significantly improves the accuracy of the results. Increasing both of the numbers of polynomials and crack functions up to I, J and $\overline{N}$ larger than 7 yield accurate numerical results that converge to at least 3 significant figures. In Table 1, the convergent results show excellent agreement with those of Stahl and Keer [2], and are slightly smaller than the latter. This is because Stahl and Keer [2] adopted the classical plate theory, which ignores the shear deformation and rotary inertia of the plate. Comparison of Tables 1 and 2 finds that the convergence rate of the results for a moderately thick plate (Table 2) is slightly better than that for a thin plate (Table 1).

Table 3
Convergence of frequency parameters $\omega a^2\sqrt{\rho h/D}$ for a simply supported square thin plate ($h/b=0.01$) having a horizontal internal crack with $d/a=0.6$ at $x_0/a=y_0/a=0.5$

Mode no.	No. of corner functions ($\overline{N}$)	order of polynomial ($I\times J$)						Published results
		5×5	6×6	7×7	8×8	9×9	10×10	
1(S)	0	19.74	19.73	19.73	19.73	19.73	19.73	[17.19]
	1	19.68	19.67	19.67	19.67	19.66	19.66	(17.33)
	2	19.46	19.45	19.40	19.40	19.37	19.37	
	3	17.64	17.54	17.51	17.47	17.44	17.42	
	4	17.19	17.19	17.18	17.18	17.17	17.17	
	5	17.17	17.16	17.15	17.15	17.15	17.15	
	6	17.16	17.15	17.15	17.15	17.14	17.14	
	7	17.15	17.14	17.14	17.14	17.14	17.14	
	8	17.15	17.14	17.13	17.13	17.13	17.13	
2(A)	0	49.45	49.45	49.30	49.30	49.30	49.30	[37.98]
	1	49.08	49.04	48.85	48.82	48.79	48.76	(37.75)
	2	43.63	43.00	42.76	42.43	42.23	41.96	
	3	38.38	38.18	38.16	38.12	38.10	38.08	
	4	37.94	37.92	37.89	37.87	37.86	37.83	
	5	37.83	37.82	37.80	37.79	37.78	37.77	
	6	37.79	37.78	37.77	37.75	37.74	37.73	
	7	37.77	37.75	37.75	37.72	37.71	37.71	
	8	37.74	37.73	37.72	37.70	37.69	37.69	
3(S)	0	49.45	49.45	49.30	49.30	49.30	49.30	[48.22]
	1	49.43	49.42	49.28	49.28	49.27	49.27	(48.26)
	2	49.39	49.38	49.25	49.24	49.24	49.24	
	3	49.06	48.99	48.93	48.91	48.89	48.87	
	4	48.24	48.22	48.22	48.21	48.20	48.19	
	5	48.15	48.15	48.15	48.15	48.15	48.14	
	6	48.15	48.15	48.14	48.14	48.14	48.14	
	7	48.14	48.14	48.13	48.13	48.13	48.13	
	8	48.14	48.14	48.13	48.13	48.13	48.13	
4(A)	0	79.05	79.05	78.84	78.84	78.84	78.84	[75.58]
	1	79.01	79.00	78.79	78.78	78.78	78.77	(75.23)
	2	78.83	78.79	78.64	78.61	78.61	78.58	
	3	77.07	76.81	76.55	76.44	76.41	76.34	
	4	75.56	75.43	75.43	75.41	75.41	75.39	
	5	75.41	75.38	75.37	75.35	75.35	75.34	
	6	75.37	75.35	75.35	75.32	75.32	75.31	
	7	75.35	75.34	75.33	75.31	75.31	75.30	
	8	75.32	75.32	75.31	75.30	75.29	75.28	
5(S)	0	139.1	99.93	99.93	98.54	98.54	98.52	[79.59]
	1	137.8	99.32	99.26	97.86	97.81	97.78	(80.32)
	2	106.1	96.96	96.35	95.24	94.95	94.94	
	3	83.03	81.93	81.66	80.93	80.78	80.65	
	4	79.79	79.66	79.57	79.46	79.43	79.42	
	5	79.38	79.36	79.34	79.33	79.32	79.32	
	6	79.33	79.31	79.31	79.30	79.30	79.29	
	7	79.31	79.29	79.28	79.27	79.26	79.25	
	8	79.31	79.26	79.25	79.24	79.22	79.22	

Note: [ ]: results from Stahl and Keer [2]; ( ): results from Liew et al. [10]

3.2. Internal-cracked plates

Tables 3 and 4 summarize the convergence studies of the first five nondimensional frequency parameters, $\omega a^2\sqrt{\rho h/D}$, for square plates having centrally located horizontal internal cracks ($x_0/a=0.5$, $y_0/b=0.5$ and $\alpha=0^o$) with d/a=0.6. Table 3 considers a thin plate (h/b=0.01) with simple supports, while Table 4 is for a thick plate (h/b=0.1) with cantilevered boundary conditions. The results are obtained using 5×5, 6×6, …,10×10 orthogonal polynomials in conjunction with sets of crack functions with $\overline{N}$=0, 1, 2, 3,…,8 in Eqs. (10) for each of ψ_x, ψ_y and w.

As observed in the convergence studies for side-cracked plates, adding the crack functions in Eqs. (10) into the admissible functions considerably enhances the accuracy of the numerical solutions. The numerical results monotonically converge from the upper bounds as the number of polynomials and crack functions increases. The excellent agreement between the convergent results and the results of Stahl and Keer [2] in Table 3 demonstrates the validity of the present solutions for plates with internal cracks. Using polynomials with I and J larger than 8 and crack functions with $\overline{N}$ larger than 6 gives results which are exact to at least 3 significant figures.

Table 4
Convergence of frequency parameters $\omega a^2\sqrt{\rho h/D}$ for a cantilevered square plate with a horizontal central internal crack ($x_0/a=y_0/a=0.5$, $d/a=0.6$, $h/a=0.1$)

Mode no.	No. of corner functions ($\overline{N}$)	Order of polynomial ($I\times J$)				
		5×5	6×6	7×7	8×8	9×9
1(S)	0	3.433	3.433	3.431	3.431	3.431
	1	3.430	3.429	3.427	3.427	3.426
	2	3.424	3.423	3.421	3.421	3.421
	3	3.422	3.421	3.420	3.420	3.419
	4	3.420	3.419	3.418	3.418	3.418
	5	3.419	3.418	3.418	3.418	3.418
	6	3.418	3.418	3.418	3.418	3.418
	7	3.418	3.418	3.418	3.418	3.418
	8	3.418	3.418	3.418	3.418	3.418
2(A)	0	8.170	8.091	8.088	8.063	8.063
	1	8.092	7.955	7.953	7.949	7.948
	2	7.945	7.924	7.922	7.882	7.881
	3	7.929	7.905	7.902	7.877	7.877
	4	7.897	7.880	7.878	7.875	7.875
	5	7.879	7.877	7.876	7.872	7.872
	6	7.877	7.873	7.873	7.872	7.872
	7	7.872	7.872	7.872	7.872	7.871
	8	7.872	7.872	7.871	7.871	7.871
3(S)	0	20.17	20.11	20.09	20.09	20.08
	1	20.14	20.09	20.06	20.06	20.05
	2	20.03	20.00	19.98	19.97	19.95
	3	19.93	19.92	19.88	19.88	19.87
	4	19.89	19.88	19.87	19.86	19.86
	5	19.87	19.87	19.86	19.86	19.85
	6	19.86	19.86	19.85	19.85	19.85
	7	19.86	19.85	19.85	19.85	19.85
	8	19.85	19.85	19.85	19.85	19.85
4(A)	0	25.81	25.68	25.51	25.51	25.49
	1	23.23	23.16	22.98	22.94	22.79
	2	21.38	21.28	21.21	21.20	21.10
	3	20.86	20.84	20.80	20.80	20.78
	4	20.77	20.76	20.75	20.75	20.74
	5	20.74	20.74	20.74	20.74	20.73
	6	20.74	20.73	20.73	20.73	20.73
	7	20.73	20.73	20.73	20.73	20.73
	8	20.73	20.73	20.73	20.73	20.73
5(S)	0	28.60	28.35	28.30	28.25	28.24
	1	27.58	27.18	27.09	26.95	26.92
	2	26.49	26.34	26.28	26.26	26.25
	3	26.24	26.16	26.15	26.13	26.13
	4	26.16	26.14	26.13	26.11	26.11
	5	26.13	26.12	26.11	26.10	26.10
	6	26.11	26.10	26.10	26.10	26.10
	7	26.10	26.10	26.10	26.10	26.10
	8	26.10	26.10	26.10	26.10	26.10

4. Frequencies and mode shapes

After the correctness and accuracy of the proposed approach was verified by performing the convergence studies, this approach was further applied to study the effects of location, length and orientation of cracks on the free vibration frequencies and mode shapes of simply supported and cantilevered rectangular plates. Only plates with h/b=0.1 are considered herein.

4.1. Side-cracked rectangular plates

Table 5 presents the first five nondimensional frequency parameters $\omega a^2\sqrt{\rho h/D}$ for thick, simply supported rectangular plates (a/b=2) with side cracks of various lengths (d/b=0.1, 0.2,…,0.6), orientations (α=90°and 135°), and locations (c_x/a=0.25 and 0.5) (Fig. 1b), while Table 6 lists the results for cantilevered rectangular plates. The results for plates with crack

Table 5
Frequency parameters $\omega a^2\sqrt{\rho h/D}$ for simply supported rectangular plates with side cracks (a/b=2, h/b=0.1), as in Fig. 1b.

α	c_x/a	d/b	Mode				
			1	2	3	4	5
		0	48.26	76.23	121.4	156.3	181.8
90°	0.5	0.1	48.26	76.10	121.4	156.3	181.4
		0.2	48.22	75.92	121.1	156.1	180.7
		0.3	48.10	75.68	120.2	155.6	178.8
		0.4	47.85	75.17	118.2	155.0	172.1
		0.5	47.44	73.98	115.2	154.8	156.9
		0.6	46.91	71.49	111.9	138.2	154.8
90°	0.25	0.1	48.23	76.22	121.3	156.2	181.6
		0.2	48.18	76.11	121.0	155.7	180.2
		0.3	48.08	75.70	120.3	155.7	180.0
		0.4	47.90	74.84	118.5	155.0	175.3
		0.5	47.58	73.51	114.8	152.5	163.6
		0.6	47.07	71.86	107.5	142.0	157.3
135°	0.25	0.1	48.22	76.22	121.3	156.1	181.6
		0.2	48.07	76.17	121.0	155.4	180.6
		0.3	47.75	76.00	120.3	153.4	178.6
		0.4	47.17	75.67	118.9	150.2	176.1
		0.5	46.30	75.08	116.1	146.9	173.4
		0.6	45.15	74.08	111.3	144.8	165.0

Table 6
Frequency parameters $\omega a^2\sqrt{\rho h/D}$ for cantilevered rectangular plates with side cracks (a/b=2, h/b=0.1), as in Fig. 1b, with x=0 clamped.

α	c_x/a	d/b	Mode				
			1	2	3	4	5
		0	3.422	14.18	21.09	45.72	58.00
90°	0.5	0.1	3.413	14.10	20.86	45.44	57.84
		0.2	3.390	13.84	20.35	44.75	57.03
		0.3	3.352	13.37	19.63	43.66	54.90
		0.4	3.296	12.72	18.77	41.80	51.33
		0.5	3.219	11.89	17.81	38.58	48.28
		0.6	3.114	10.92	16.80	34.68	46.74
90°	0.25	0.1	3.390	14.08	21.05	45.49	57.57
		0.2	3.314	13.71	20.91	44.69	56.57
		0.3	3.204	13.08	20.63	43.36	55.23
		0.4	3.063	12.20	20.20	41.67	53.78
		0.5	2.892	11.11	19.65	39.98	52.34
		0.6	2.693	9.881	19.03	38.59	50.92
135°	0.25	0.1	3.406	14.12	21.06	45.60	57.72
		0.2	3.372	13.92	20.92	45.11	56.92
		0.3	3.330	13.56	20.57	44.13	55.82
		0.4	3.283	13.05	19.93	42.60	54.81
		0.5	3.233	12.38	18.97	40.69	54.08
		0.6	3.182	11.55	17.79	38.75	53.38

length $d/b \le 0.3$ were obtained using polynomials with 9×9 terms and crack functions with $\overline{N} = 7$ in Eqs. (9) yielding a total of 453 degrees of freedom in the resulting eigenvalue problems in the Ritz method; the results for $d/b \ge 0.4$ were obtained using polynomials with 9×9 terms and crack functions with $\overline{N} = 8$ in Eqs. (9) resulting in a total of 507 degrees of freedom. Extensive convergence studies, not presented here, indicate that the frequencies are exact to at least three significant figures.

As expected, the frequency of each mode reduces as the crack length increases because increasing the crack length reduces the stiffness of the plate. A crack with d/a=0.6 can reduce the frequencies up to more than 14% and 30% for simply supported plates and cantilevered plates, respectively. Moving the crack from c_x/a=0.25 to 0.5 increases the frequencies of the first two modes and reduces the frequency of the third mode for cantilevered plates. Changing the crack orientation from α=90° to 135° increases the frequencies of the first two modes, the fourth and the fifth modes for cantilevered plates, while the change of α reduces the frequency of the first mode and increases the frequencies of the second and third modes for simply supported plates. A small crack d/a=0.1 in various locations and orientations results in frequencies which slightly differ from those for intact plates, with differences of less than 0.22% and 1.1% for simply supported plates and cantilevered plates, respectively.

Figs. 3 and 4, respectively, display nodal patterns for simply supported and cantilevered rectangular plates having side cracks at different locations (c_x/a=0.25 and 0.5), with various lengths (d/b=0.2 and 0.6) and orientations (α=90°and 135°). In these figures, dashed lines denote the nodal lines where transverse displacement equals zero, and solid lines represent non-zero contours. The crack destroys the symmetry of plate with respect to the horizontal line passing the center of the plate. Therefore, the nodal lines for the cracked plates are no longer symmetric to the horizontal line. Nevertheless, the nodal lines for a simply supported plate with a vertical crack at c_x/a=0.5 are still symmetric with respect to the vertical line including the crack. The nodal patterns for the higher modes (i.e., the fourth and fifth modes) are rather sensitive to the location, length and orientation of the crack.

4.2. Internal-cracked square plates

Table 7 presents the first five nondimensional frequency parameters $\omega a^2\sqrt{\rho h/D}$ for simply supported square plates with centrally located cracks of various lengths (d/b=0.1, 0.2,…, 0.6) and orientations (α=0°, 15°, 30° and 45°) (Fig. 2), while Table 8 shows the results for cantilevered square plates. The results for plates with crack length $d/b \le 0.3$ were obtained using polynomials with 8×8 terms and crack functions with $\overline{N} = 5$ in Eqs. (10) yielding a total of 432 degrees of freedom; the results for $d/b \ge 0.4$ were obtained using polynomials with 8×8 terms and crack functions with $\overline{N} = 6$ in Eqs. (10) resulting in a total

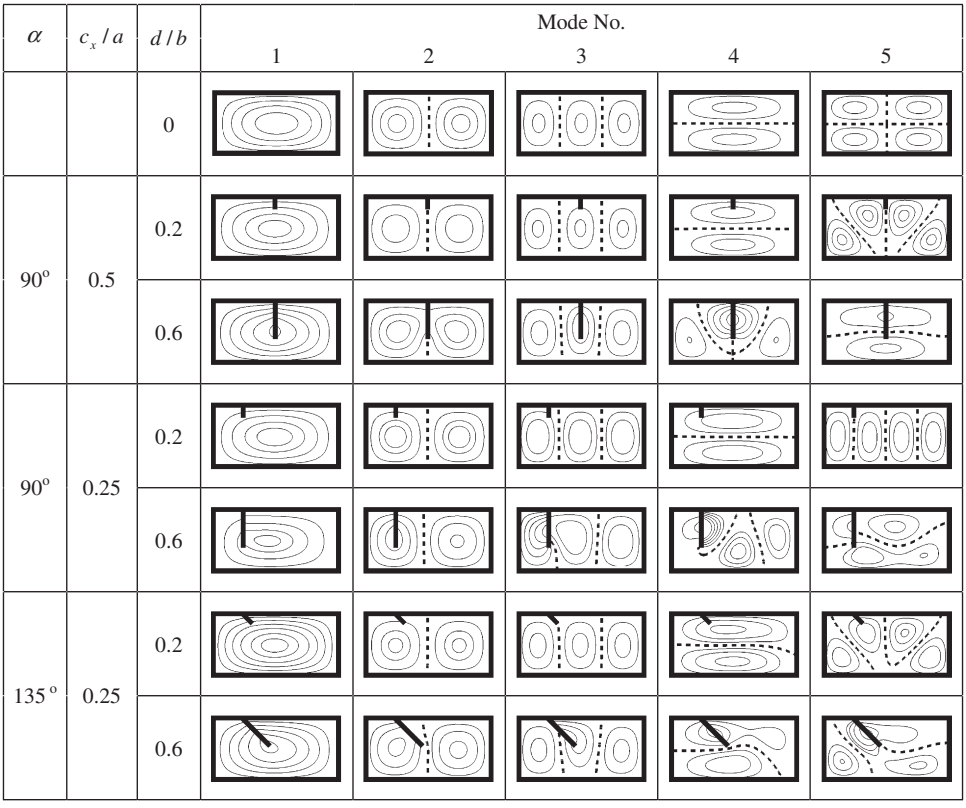

Fig. 3. Nodal patterns for simply supported rectangular plates with side cracks (a/b=2, h/b=0.1).

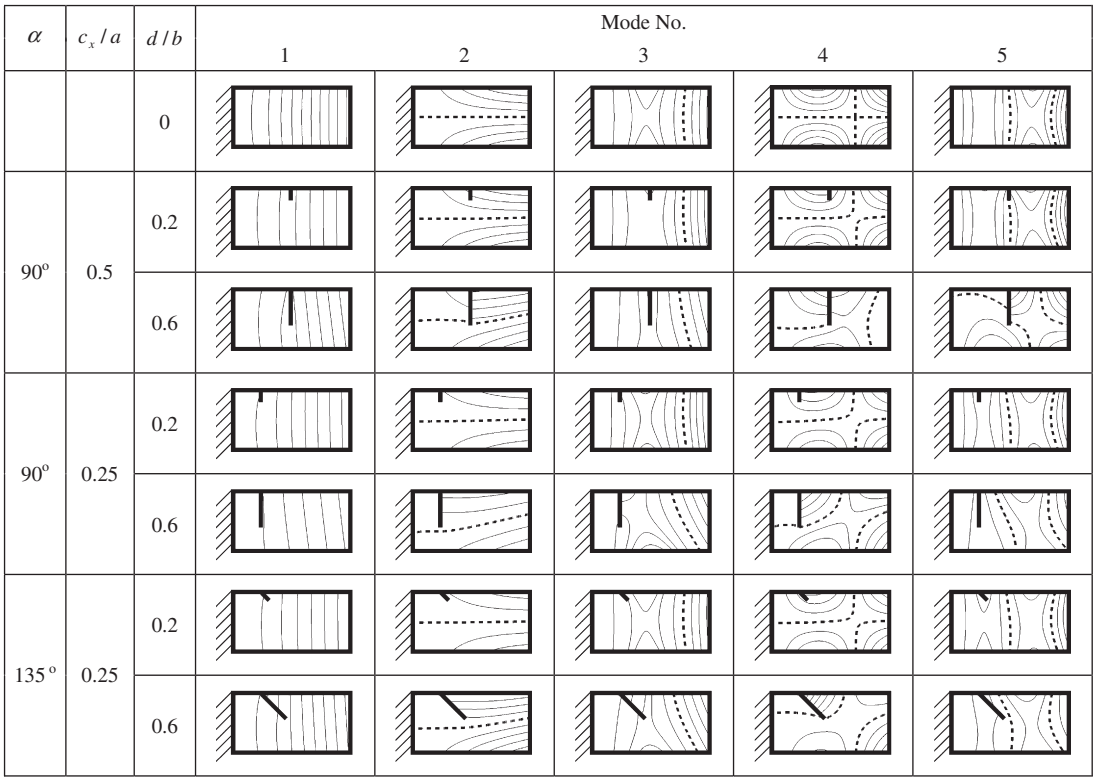

Fig. 4. Nodal patterns for cantilevered rectangular plates with side cracks (a/b=2, h/b=0.1).

Table 7
Frequency parameters $\omega a^2\sqrt{\rho h/D}$ for simply supported square plates (h/b=0.1) with central internal cracks ($x_0/a = y_0/a = 0.5$).

α	d/a	Mode				
		1	2	3	4	5
	0	19.06	45.45	45.45	69.72	84.93
0°	0.1	18.86	45.35	45.45	69.56	83.20
	0.2	18.43	44.84	45.41	69.28	79.70
	0.3	17.88	43.46	45.28	68.91	76.00
	0.4	17.29	40.65	45.02	68.22	72.87
	0.5	16.72	36.43	44.62	66.81	70.50
	0.6	16.23	31.65	44.10	64.16	68.77
15°	0.1	18.85	45.35	45.44	69.54	83.13
	0.2	18.44	44.85	45.41	69.19	80.06
	0.3	17.85	43.47	45.28	68.52	76.61
	0.4	17.24	40.65	44.98	67.42	74.11
	0.5	16.66	36.40	44.51	65.90	72.09
	0.6	16.13	31.67	43.91	63.78	69.88
30°	0.1	18.88	45.35	45.44	69.54	83.59
	0.2	18.43	44.84	45.40	68.99	80.60
	0.3	17.85	43.44	45.24	67.96	78.07
	0.4	17.21	40.63	44.88	66.47	76.49
	0.5	16.55	36.42	44.29	64.81	74.48
	0.6	15.92	31.69	43.48	63.16	69.55
45°	0.1	18.87	45.35	45.44	69.52	83.53
	0.2	18.43	44.84	45.40	68.89	80.93
	0.3	17.85	43.44	45.22	67.71	78.87
	0.4	17.18	40.62	44.83	66.07	77.88
	0.5	16.49	36.42	44.17	64.39	74.22
	0.6	15.80	31.69	43.25	62.87	69.19

Table 8
Frequency parameters $\omega a^2\sqrt{\rho h/D}$ for cantilevered square plates (h/b=0.1) with central internal cracks ($x_0/a=y_0/a=0.5$).

α	d/a	Mode				
		1	2	3	4	5
	0	3.430	8.057	20.08	25.49	28.22
0°	0.1	3.430	8.038	20.08	25.21	28.21
	0.2	3.429	8.005	20.08	24.58	28.16
	0.3	3.428	7.971	20.08	23.72	28.02
	0.4	3.426	7.937	20.07	22.71	27.71
	0.5	3.422	7.904	20.03	21.65	27.13
	0.6	3.418	7.871	19.85	20.73	26.10
15°	0.1	3.430	8.035	20.07	25.21	28.22
	0.2	3.428	8.000	20.05	24.64	28.17
	0.3	3.424	7.949	20.04	23.79	28.04
	0.4	3.419	7.900	20.02	22.84	27.77
	0.5	3.413	7.842	20.00	21.85	27.26
	0.6	3.402	7.774	19.94	20.85	26.31
30°	0.1	3.428	8.036	20.04	25.28	28.22
	0.2	3.422	7.987	19.97	24.75	28.18
	0.3	3.414	7.907	19.90	24.07	28.09
	0.4	3.400	7.822	19.80	23.05	27.90
	0.5	3.382	7.711	19.70	22.44	27.55
	0.6	3.356	7.576	19.58	21.62	26.86
45°	0.1	3.428	8.041	20.00	25.33	28.22
	0.2	3.415	7.986	19.84	24.96	28.20
	0.3	3.403	7.922	19.69	24.51	28.15
	0.4	3.373	7.795	19.36	23.86	28.06
	0.5	3.336	7.648	19.07	23.26	27.86
	0.6	3.287	7.395	18.64	22.46	27.38

of 516 degrees of freedom. The frequencies of intact plates (i.e., d/b=0) were obtained using only orthogonal polynomials with I=J=10. The frequencies are exact to at least three significant figures.

Increasing the crack length reduces the frequency of each mode. The frequencies of the third mode in Table 7 are less sensitive to the crack length than the other modes, and the reduction in frequency is less than 5% even when the crack length d/b=0.6. The frequencies of the fourth mode in Table 8 are affected the most by the crack length among the first five modes. A small crack (d/b=0.1) reduces the frequencies of the first four modes for simply supported cracked plates and the frequencies of the first five modes for cantilevered cracked plates by only less than 1.1%. Changing the crack orientation from α=0°, 15°, 30°, and to 45° generally reduces the frequencies of the first, third and fourth modes in Table 7 and the first three modes in Table 8. It is seen that the frequencies for simply supported cracked plates are more affected by the length and orientation of crack than are those for cracked cantilevered plates, except for the fourth mode.

Figs. 5 and 6 depict the nodal patterns of the first five modes for some of the plates considered in Tables 7 and 8, respectively. Contours of the transverse displacement are given by the solid lines, while the dashed lines denote the nodal lines. For square plates with center cracks ($(x_0/a,y_0/b)$=(0.5, 0.5)) on one of their symmetry axes, the vibration mode shapes are still either symmetric or anti-symmetric to the axes. This is found in the nodal patterns for α=0° and 45° in Fig. 5 and for α=0° in Fig. 6. A crack with $\alpha\neq0^o$ makes the otherwise crossing nodal lines for an intact plate veer with each other (i.e., the fourth mode in Fig. 5 and the fifth mode in Fig. 6).

5. Concluding remarks

This work has been demonstrated that accurate nondimensional frequencies of thick, cracked rectangular plates can be obtained by means of the Ritz method with appropriate admissible functions. In the present solutions, the admissible functions for bending rotations (ψ_x and ψ_y) and transverse displacement (w) in Mindlin plate theory consist of mathematically complete polynomials and new sets of functions (crack functions) proposed to properly describe the important features of true solutions along a crack. The proposed new sets of functions appropriately represent the stress singularity behaviors around a crack tip and elucidate the discontinuities of transverse displacement and bending rotations across the crack. The efficiency of the proposed crack functions has been substantiated through extensive convergence studies of nondimensional frequencies for simply supported and cantilevered rectangular plates with side cracks and internal cracks. The convergent results for simply supported cracked thin plates (h/b=0.01) agree excellently with previously published results based on the classical thin plate theory, confirming the correctness and accuracy of the present solutions.

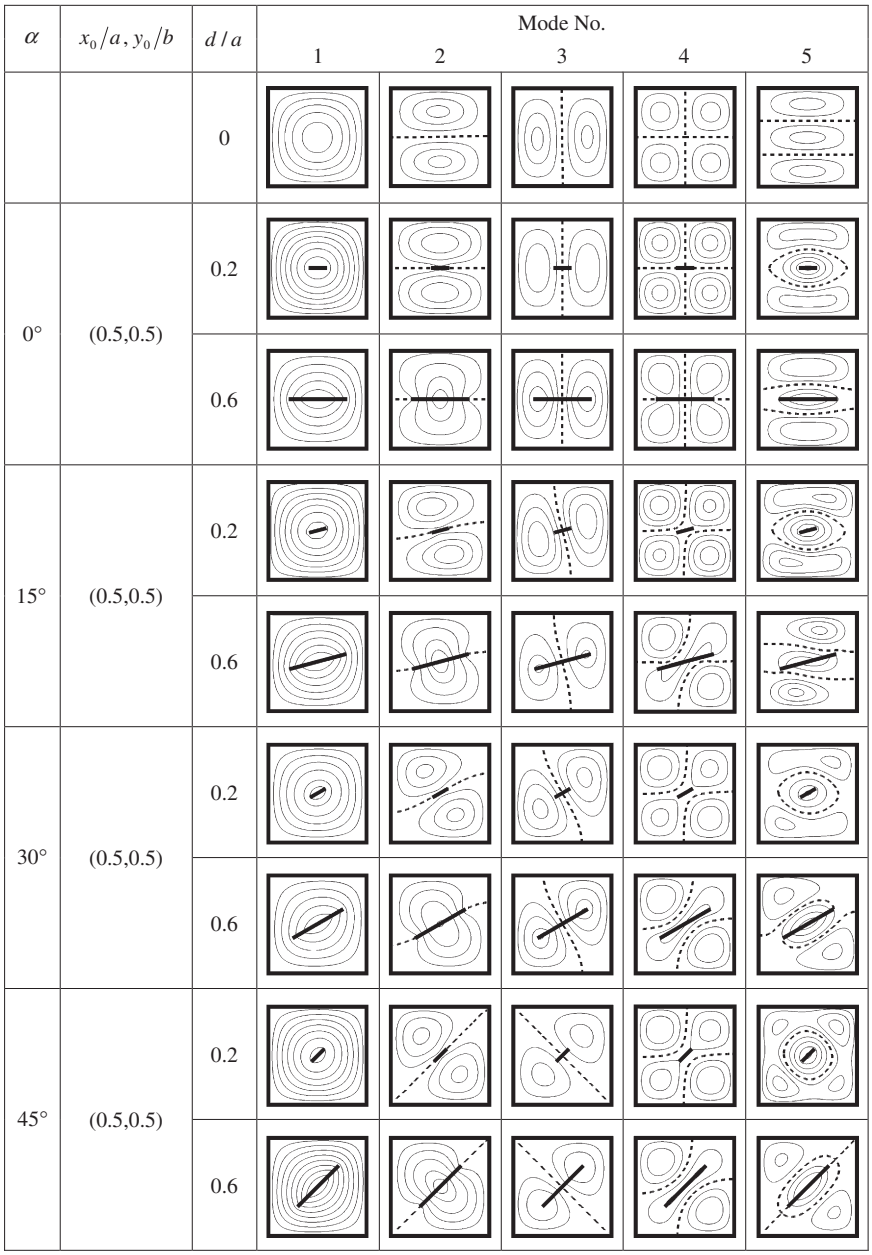

Fig. 5. Nodal patterns for simply supported square plates with central internal cracks.

Accurate nondimentional frequency data and nodal patterns and contours of transverse displacement have been provided for simply supported and cantilevered rectangular thick plates ($h/b=0.1$) with side cracks or internal cracks of various lengths ($d/b=0.1, 0.2, \ldots, 0.6$), orientations ($\alpha=0^\circ, 15^\circ, 30^\circ, 45^\circ, 90^\circ$ and 135°) and locations ($c_x/a=0.25$ and 0.5). These results are exact to at least three significant figures and are the first ones shown in the literature. These data illustrate the effects of crack length, orientation and location on the natural frequencies. A small crack (i.e., $d/a=0.1$) only slightly reduces the frequencies of the first five modes.

Although the present approach employs the Ritz method that is a traditional and popular method in analyzing the free vibrations of plates with geometry not too complicated, this work has proposed new sets of crack functions to promote the capabilities of the Ritz method in accurately finding the frequencies and nodal patterns of cracked plates. It will be interesting to see how the proposed approach is applied to determine stress intensity factors of plates under various loading conditions. The proposed crack functions can also be used in numerical methods other than the Ritz method, such as the element-free Galerkin method and meshless collocation method to study the static and dynamic problems of cracked plates with complicated geometry.

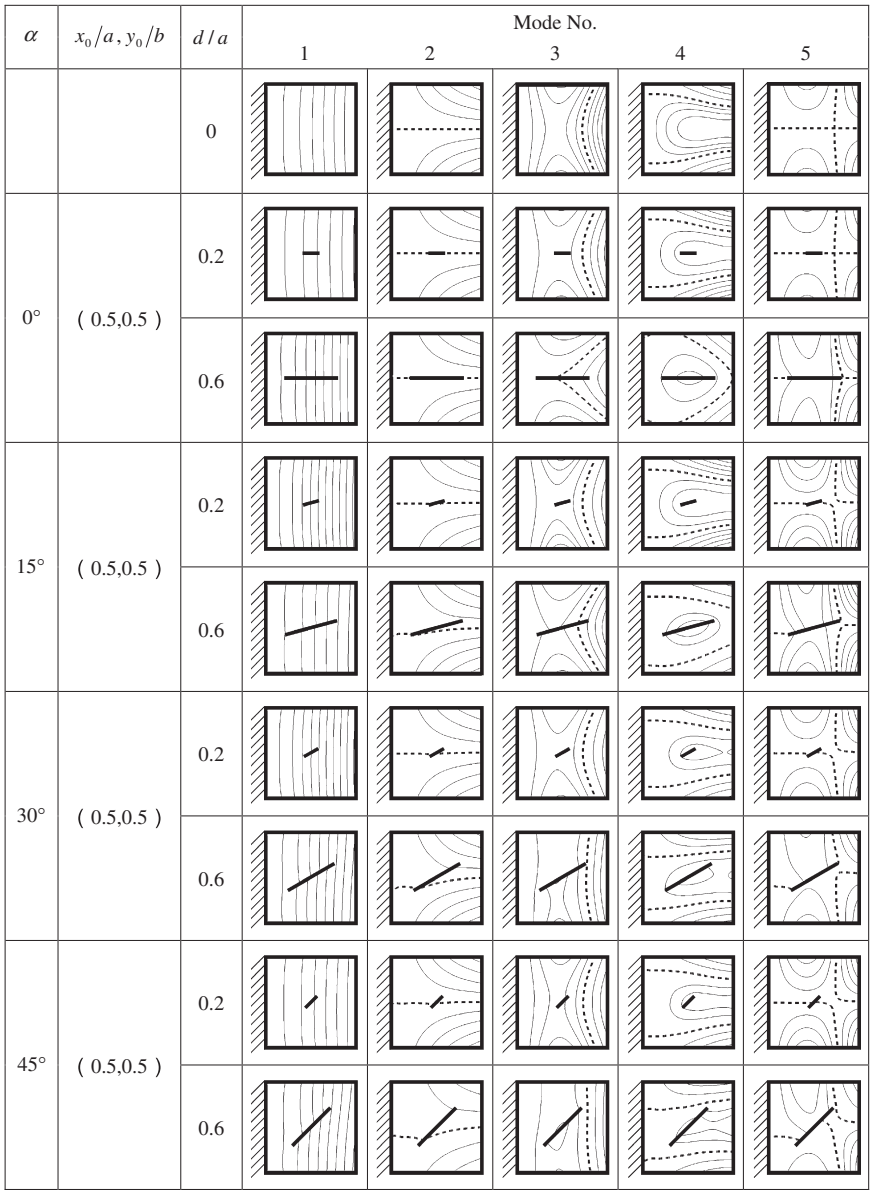

Fig. 6. Nodal patterns for cantilevered square plates (h/b=0.1) with central internal cracks.

Acknowledgement

This work reported herein was supported by the National Science Council, Taiwan through research Grant no. NSC98-2221-E-009-075-MY3. This support is gratefully acknowledged.

References

[1] P.P. Lynn, N. Kumbasar, Free vibrations of thin rectangular plates having narrow cracks with simply supported edges, *Developments in Mechanics*, 4, *Proceedings of the 10th Midwestern Mechanics Conference*, Colorado State University, Fort Collins, CO, August 21–23, 1967, pp. 911–928.
[2] B. Stahl, L.M. Keer, Vibration and stability of cracked rectangular plates, *International Journal of Solids and Structures* 8 (1) (1972) 69–91.
[3] B.D. Aggarwala, P.D. Ariel, Vibration and bending of a cracked plate, *Rozprawy Inzynierskie* 29 (2) (1981) 295–310.
[4] K. Neku, Free vibration of a simply-supported rectangular plate with a straight through-notch, *Bulletin of the Japan Society of Mechanical Engineers* 25 (199) (1982) 16–23.
[5] R. Solecki, Bending vibration of a simply supported rectangular plate with a crack parallel to one edge, *Engineering Fracture Mechanics* 18 (6) (1983) 1111–1118.
[6] Y. Hirano, K. Okazaki, Vibration of cracked rectangular plates, *Bulletin of the Japan Society of Mechanical Engineers* 23 (179) (1980) 732–740.

[7] G.L. Qian, S.N. Gu, J.S. Jiang, A finite element model of cracked plates and application to vibration problems, *Computers and Structures* 39 (5) (1991) 483–487.
[8] M. Krawczuk, Natural vibrations of rectangular plates with a through crack, *Archive of Applied Mechanics* 63 (7) (1993) 491–504.
[9] J. Yuan, S.M. Dickinson, The flexural vibration of rectangular plate systems approached by using artificial springs in the Rayleigh–Ritz method, *Journal of Sound and Vibration* 159 (1) (1992) 39–55.
[10] K.M. Liew, K.C. Hung, M.K. Lim, A solution method for analysis of cracked plates under vibration, *Engineering Fracture Mechanics* 48 (3) (1994) 393–404.
[11] C.S. Huang, A.W. Leissa, Vibration analysis of rectangular plates with side cracks via the Ritz method, *Journal of Sound and Vibration* 323 (3–5) (2009) 974–988.
[12] M. Bachene, R. Tiberkak, S. Rechak, Vibration analysis of cracked plates using the extended finite element method, *Archive of Applied Mechanics* 79 (2009) 249–262.
[13] C.C. Ma, C.H. Huang, Experimental and numerical analysis of vibrating cracked plates at resonant frequencies, *Experimental Mechanics* 41 (1) (2001) 8–18.
[14] K. Maruyama, O. Ichinomiya, Experimental study of free vibration of clamped rectangular plates with straight narrow slits, *JSME International Journal Series III* 32 (2) (1989) 187–193.
[15] C.C. Ma, D.M. Hsieh, Full-field experimental investigations on resonant vibration of cracked rectangular cantilever plates, *AIAA Journal* 39 (12) (2001) 2419–2422.
[16] H.P. Lee, S.P. Lim, Vibration of cracked rectangular plates including transverse shear deformation and rotary inertia, *Computers & Structures* 49 (4) (1993) 715–718.
[17] C.S. Huang, A.W. Leissa, M.J. Chang, Vibrations of skewed cantilevered triangular, trapezoidal and parallelogram Mindlin plates with considering corner stress singularities, *International Journal for Numerical Methods in Engineering* 62 (13) (2005) 1789–1806.
[18] R.B. Bhat, Natural frequencies of rectangular plates using characteristic orthogonal polynomials in Rayleigh–Ritz method, *Journal of Sound and Vibration* 102 (4) (1985) 493–499.
[19] C.S. Huang, Stress singularities at angular corners in first-order shear deformation plate theory, *International Journal of Mechanical Sciences* 45 (2003) 1–20.